Characterisation and Analysis of the Impact of Cold Jointing in Cemented Paste Backfill stopes

Bre-Anne Sainsbury[1], David Sainsbury[2], Dean Harty[3], Florencio Felipe[4], Marc Ruest[5] and David McLoughney[6]

[1] Deakin University, Waurn Ponds, VIC, Australia, breanne.sainsbury@deakin.edu.au
[2] Geotechnica, Melbourne, VIC, Australia, david.sainsbury@geotechnica.com.au
[3] Northern Star Resources, Perth, WA, Australia, DHarty@nsrltd.com
[4] Agnico Eagle Mines Limited, Fosterville, VIC, Australia, Florencio.Felipe@agnicoeagle.com
[5] Lundin Mining, Vancouver, BC, Canada, marc.ruest@lundinmining.com
[6] BHP, Adelaide, SA, Australia, david.mcloughney@bhp.com

Abstract

The presence of discontinuities (cold, batch, flow, slick, slurry, or water joints) within cemented paste backfill (CPB) are known to have an impact on the stability of underhand stope exposures. Currently, there is limited understanding of the mechanical properties of these internal discontinuities. A geomechanical testing program has been completed that measures the tension response of synthetic discontinuities that have been created in cemented paste backfill in the laboratory. Three-dimensional modelling has been completed to demonstrate the effect on stability from the presence of discontinuities within a CPB fill mass that create backfill beams. It has been shown that when a backfill beam height is > 70% of the span width, its presence is unlikely to cause instability issues. As such, it is advised that this value be considered as the minimum thickness of a continuous plug pour to minimise dilution.

Key words: cold joint, slick joint, slurry joint, strength, cemented paste backfill (CPB), backfill beam

Introduction

Placement of CPB at many underground mines is, in many cases, discontinuous due to interruptions and delays in operational shift schedules, plant batching procedures, and maintenance required on the reticulation system. This discontinuous filling can result in the formation of planes of weakness (discontinuities) between CPB pours which are referred to as cold, batch, or flow joints. The frequency of discontinuities within the fill mass can be further increased during flushing of the reticulation system whereby water or low cement 'slick' products are flushed through the pipelines; these joints are sometimes referred to as slurry, slick, or water joints. The typical discontinuous fill profile of a stope that creates backfill beams (Figure 1) has previously been documented by Hasan et al., (2014).

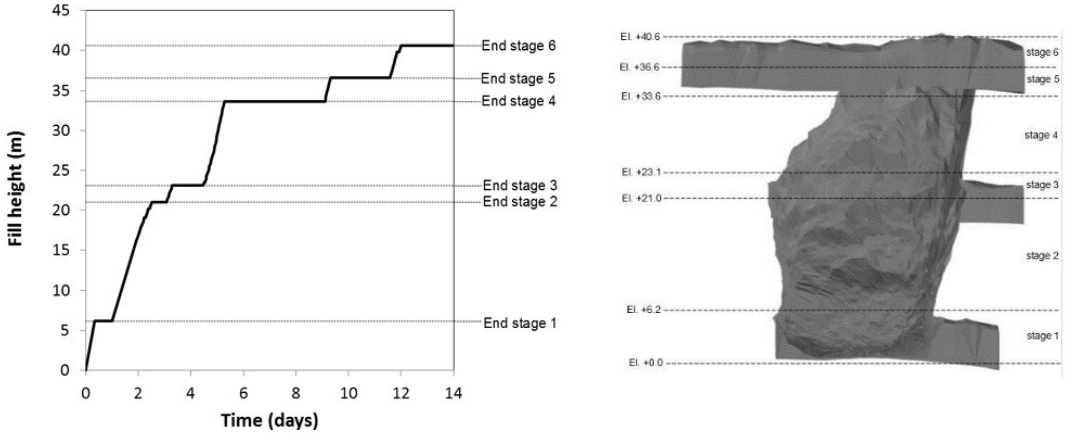

Figure 1. Typical discontinuous filling sequence of a stope (modified after Hasan et al., 2014).

The presence of any of these discontinuities (cold, batch, flow, slick, slurry, or water joints) within CPB are known to have an impact on the stability behaviour of underhand stope exposures (Li et al., 2014). They have previously been observed to be a contributor to an underhand backfill failure at the Lucky Friday Mine (Johnson et al., 2015), and dilution at the Henty Mine (Sainsbury and Cai, 2001) and Fosterville Gold Mine (Farrington, 2020). Although they are frequently observed during exposure (Figure 2), there is limited understanding of their mechanical properties and impact on CPB exposure design (Grabinsky et al., 2022).

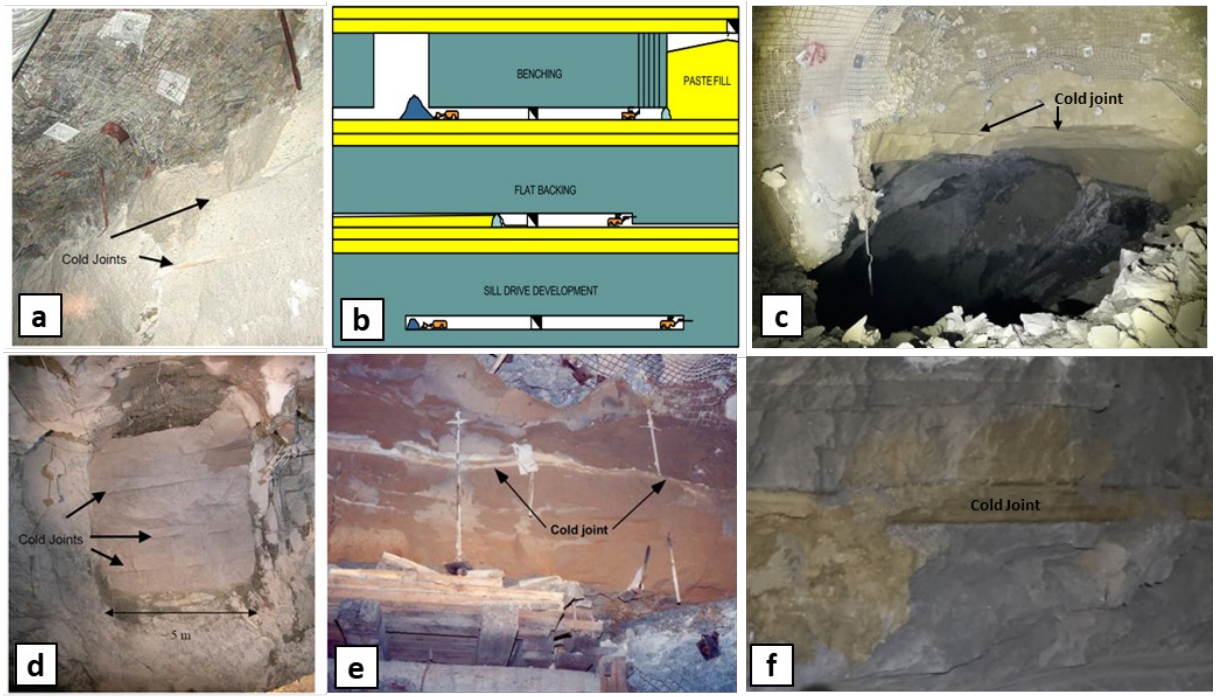

Figure 2. Cold joints observed in paste fill exposures at (a,b) Henty Mine (modified after Sainsbury and Cai, 2001), (c) Fosterville Gold Mine (modified after Farrington, 2020), (d) Kanowna Bell Mine, (e) Lucky Friday Mine (modified after Johnson et al., 2015), and (f) Kibali Mine.

An attempt was made by Johnson et al. (2015) to characterise the strength of cold joints at the Lucky Friday Mine (Figure 3). Cold joints retrieved from *in situ* samples were characterised with a mean direct tension strength of 0.16 MPa. This equates to 65% the homogenous direct tension strength and 4% of the measured CPB UCS. However, due to limitations associated with sample retrieval and testing, the results were considered inconclusive.

Exposure stability modelling that is used to define the required CPB strength and exposure size typically either neglects these internal features (Sainsbury and Urie, 2007; Tesarik et al. 2007) or applies conservative tension strength values of 0 kPa tension (Sainsbury and Cai, 2001). In either case, the resulting design may result in dilution (due to an under-estimation of strength required) and/or additional operational costs (increased binder addition) that is not necessary.

To provide some initial guidance on the strength of CPB discontinuities, a geomechanical testing program was completed the quantifies the tensile response of synthetic discontinuities that were created in the laboratory. The measured response was used as direct input to numerical exposure stability analyses that considers their impact on stability and strength requirements for variations in stope spans and backfill beam heights.

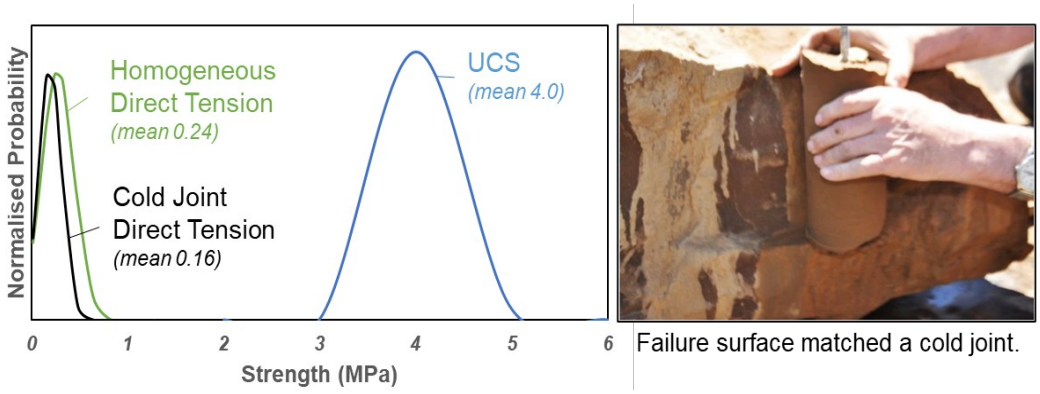

Figure 3. Characterisation of cold joint strength modified after Johnson et al. (2015).

Laboratory Testing

CPB samples were prepared in the laboratory in small batches (< 7 kg) using mine specific filter cake, binder, and water from Northern Star Resources Carouse Dam, Kanowna Belle and Thunderbox Mines, Agnico Eagle's Fosterville Gold Mine (formerly Kirkland Lake Gold), and BHPs Prominent Hill Mine (formerly Oz Minerals). Samples ranged in binder content from 1.5–9% and pulp solids from 60–85%.

For each batch, the UCS was determined to provide a control reference for the direct tension responses. For each UCS strength reported, at least 3 samples were used to determine an average reference value. The direct tension response was established for a range of UCS values based on the direct measurement procedure documented by Sainsbury et al. (2024) that was based on the publications of Alhussainy et al. (2019), Guo et al. (2022) and Pan and Grabinsky (2021). Curing and testing moulds were printed in a Fortus 450mc Production System with front and back pieces cut from 2 mm Perspex to provide transparency. A bespoke tension bracket was utilised to strain the sample (Figure 4).

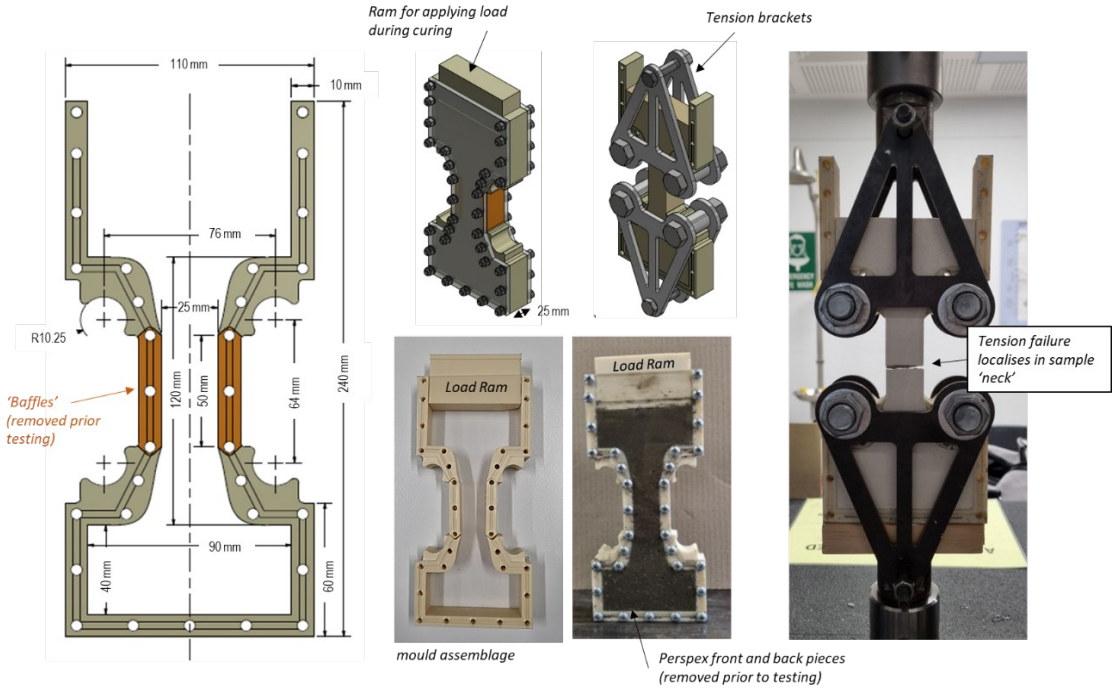

Figure 4. Direct tension mould assemblage and application.

Development of Synthetic CPB Discontinuities

Synthetic CPB discontinuities have previously been generated in the laboratory by Nasir and Fall (2008) and Koupouli et al. (2017). However, these studies considered the strength of the CPB-rock interface and not internal discontinuities.

For the range of UCS values, direct tension samples were prepared with and without synthetic joints for comparison. In relation to the synthetic joint preparation the following methodology was applied:

- **Cold/Batch joints** Moulds were half filled and cured at 23°C and 50% relative humidity (RH) for 24 hr. The same batch mix was placed on top of the early age CPB after 24 hours to complete the sample. The samples were then cured for 28 days at 23°C and 50% relative humidity prior to testing.
- **Water/Slurry/Slick joints** Moulds were half filled. For the water joints, after 10 mins, 1 mm of room temperature water was placed on top of the paste to replicate line cleaning. The samples were cured at 23°C and 50% RH for 24 hours. After this time, an additional 1 mm of water and the same batch mix was poured to complete the sample to replicate line slicking and continued placement. The samples were cured for 28 days at 23°C and 50% RH prior to testing.

Examples of the discontinuous samples after preparation and testing are provided in Figure 5. A summary of the homogeneous results are provided in Sainsbury et al., (2024).

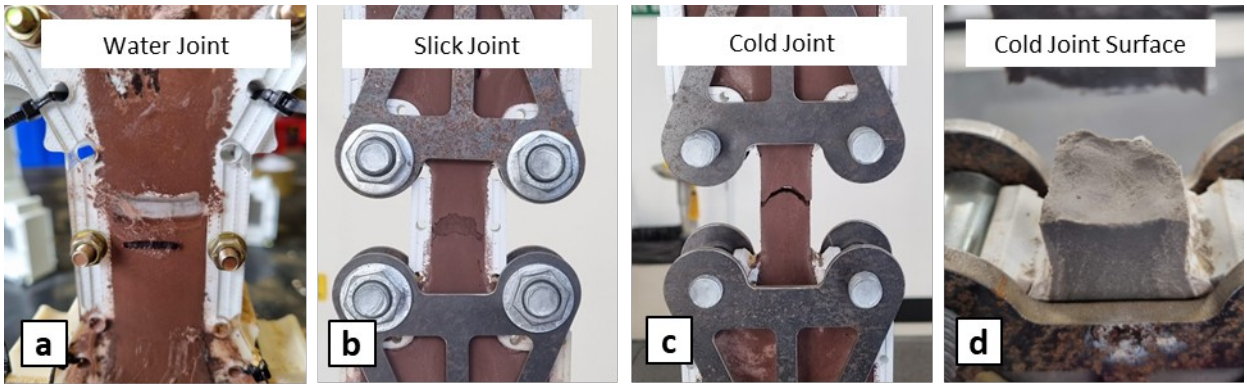

Figure 5. CPB synthetic discontinuities: a) water joint immediately after 'batching', b) slurry joint after 28 days curing, and both (c) and (d) batch/cold joint after tensile failure.

Laboratory Results

A summary of the laboratory test results is provided in Figure 6, limited to the UCS strength range 400–1600 kPa. This range is typical for mining operations (Brackebusch, 1995) and reflects the high variability in the range of solids, water and binder content. Notable outcomes of the geomechanical testing include the following:

- slick joints are stronger in tension than cold joints and provide a strength of approximately 5.6% of the UCS or 20% of the homogenous direct tension response. Consideration of the strength of the measured discontinuity strength at the Lucky Friday Mine suggests it was a water/slurry/slick joint based on the comparison to its homogenous response.
- Cold joints provide a tension strength of approximately 0.6% of the UCS or 2% of the homogenous direct tension response.

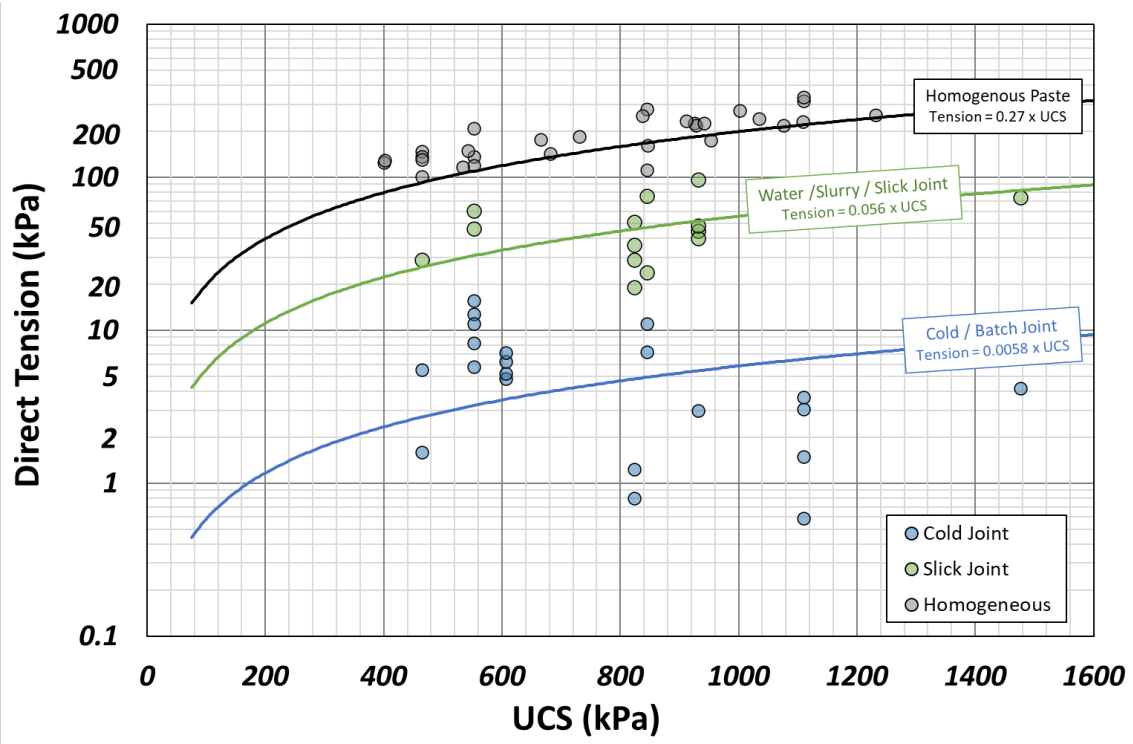

Figure 6. CPB direct tensile strength and consideration of slurry/slick and cold/batch joints.

While relatively small value, the characterisation of some tension strength is more than the conservative estimate of 0 kPa. The impact of these increased strengths on exposure stability modelling results are considered in the following section.

Numerical Analysis

Paste fill exposures created by adjacent mining must be strong enough to prevent failure of the entire fill mass and major sloughing of the vertical and underhand exposure faces. Mitchell (1983, 1991) proposed a series of analytical solutions for vertical and underhand cemented backfill exposure stability that are still often used at least for preliminary design, and which motivated subsequent empirical design methods (Pakalnis et al., 2005; Hughes, 2014). Fully employing the Mitchell solutions requires knowledge of the backfill material's UCS, modulus, and tension strength, as well as estimates of stope wall closure. Multiple authors (Oulbacha, 2014; Pagé et al., 2019; Grabinsky et al., 2022) have demonstrated that these existing approaches have limited applicability; a more general, full analysis in support of rational design will require numerical modelling that incorporates the effect of the surrounding rock mass and confining stress on the material's stiffness and mobilized strength.

To analyse the performance of paste exposures, a three-dimensional numerical modelling approach has been adopted with the FLAC^{3D} program (Itasca Consulting Group, 2022). The modelling methodology used within this report has been developed and continuously improved over a period of 23 yrs based on the design, implementation and back-analysis of cemented backfill exposures at operating mines throughout the world (Sainsbury et al., 2003; Sainsbury and Urie, 2007; Sainsbury and Sainsbury, 2014; and Shiels and Sainsbury, 2020).

Model Conditions

The numerical analysis includes the consideration of a simplified four stope sequence that includes two vertical exposures and one underhand (horizontal) exposure on Stope 1 (Figure 7). For the simplified

mining sequence, a range of stope strike lengths (10, 20 and 30 m) and backfill beam heights created by the presence of a cold joint (1, 2, 3 and 7 m above the stope floor) were considered to quantify the UCS required to maintain stability (FOS ~ 1).

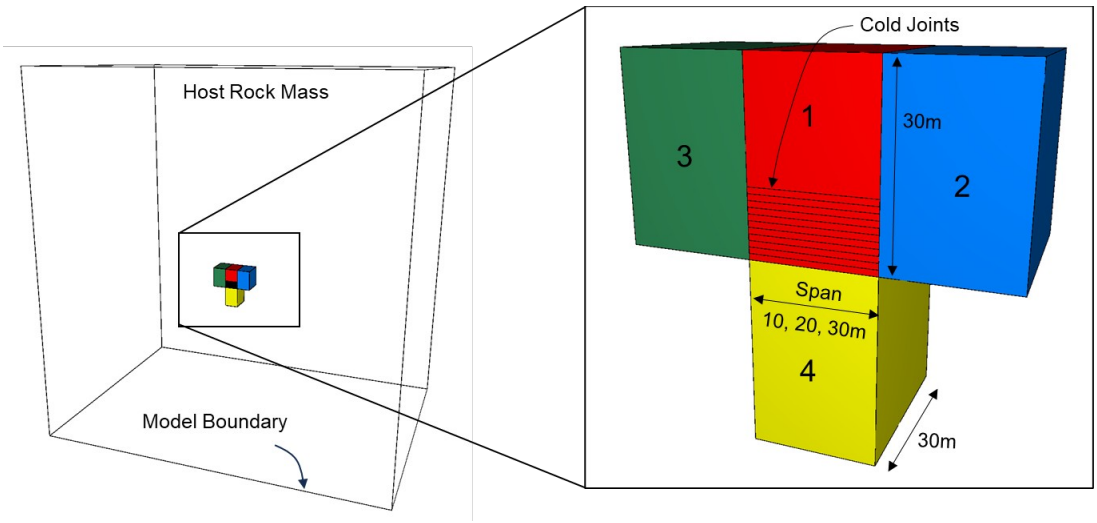

Figure 7. Model geometry and mining sequence including location of cold joints in Stope 1.

A lithostatic vertical stress profile with a horizontal stress twice this was assigned and the stopes were simulated at a depth of 700 m below the ground surface. These stress conditions are representative of the *in situ* conditions at many underground stoping operations.

Material Properties

Wall rock

Due to its strain-softening nature, the stability response of paste backfill is influenced by internal stresses that are controlled by curing age and exposure. Stability is also influenced by the host rock mass that yields and converges/diverges during the mining sequence and results in both stress redistribution and displacements in the backfilled stope (Qi et al., 2022). A smaller CPB span in a more deformable host rock is most exposed to deformations. As such, the representation of the host rock mass in a numerical exposure stability model is critical. The host rock mass has been represented in the simplified model as an elastic medium with properties consistent with UCS 100 GSI 55 and *mi* 18.

Paste fill

Density, modulus and tension values for the homogeneous paste fill mass were derived based on the geomechanical database presented in Sainsbury et al. (2024) and the assigned UCS. A friction angle (Ø) of 30° was assigned to the CPB, consistent with geomechanical characterisations completed by Brummer et al. (2003), and Rankine and Sivakugan (2007). Cohesion (c) has been assigned based on Ø and UCS based on the Mohr-Coulomb (Equation 1).

$$UCS = \frac{2c\cos\emptyset}{1-\sin\emptyset} \qquad \text{Equation 1}$$

Each stope is filled with sequentially with a 2 m lift height with increasing strength and stiffness to accurately simulate the internal stress distribution within each fill mass.

Cold joints

Interfaces that are able to slip and separate have been used to represent cold joints within the numerical model. The explicit representation of the cold joint is critical in being able to accurately capture the backfill beam bond strength and flexure behaviour that analytical and implicit numerical solutions can not (Sainsbury and Sainsbury, 2017; Hu et al., 2020). Cold joint tension strengths have been determined based on the assigned UCS and direct tension test data (Figure 8). A friction angle of 30° has been assigned to the cold joints. This value represents the residual friction angle of CPB materials published by Pan et al. (2021). It is also consistent with preliminary direct shear responses observed for cold joints (Figure 8).

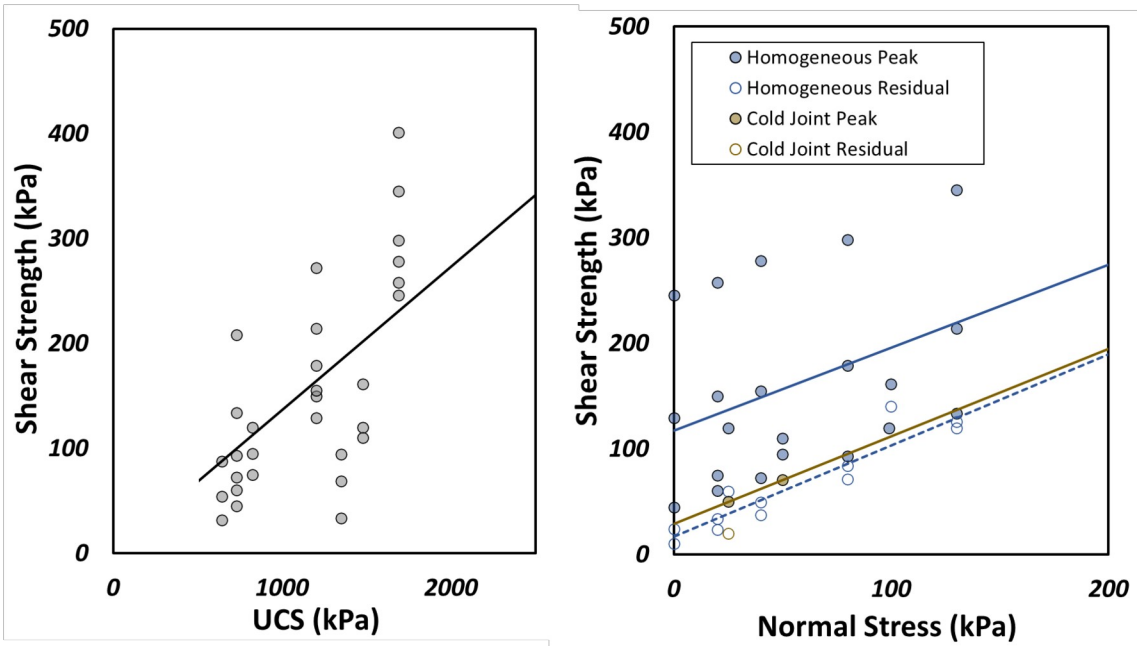

Figure 8. Shear response of paste fill cold joints. Homogenous responses are reported after Pan et al. (2021)

Cohesion values for the cold joints were determined based on the shear (τ) responses (left) generalised in Equation 2.

$$\tau = 0.14(UCS) \qquad \text{Equation 2}$$

Normal stresses in the order of 150–250 kPa were measured in an *in situ* stope (Thompson et al., 2012). Normal stress of 200 kPa was used to determine the cohesion (c) based on the direct shear results (Figure 8) and traditional Coulomb–Terzaghi shear strength Equation 3.

$$c = 0.0309(UCS) - 10.3e3 \qquad \text{Equation 3}$$

where c and UCS are quantified in Pa.

Normal and shear stiffness values of the cold joint interface were scaled based on the CPB modulus. Example results for the 20 m stope span and 1 m cold joint spacing are presented in Figure 9. For these results, a FOS of 1 has been inferred at a CPB UCS of 1850 kPa.

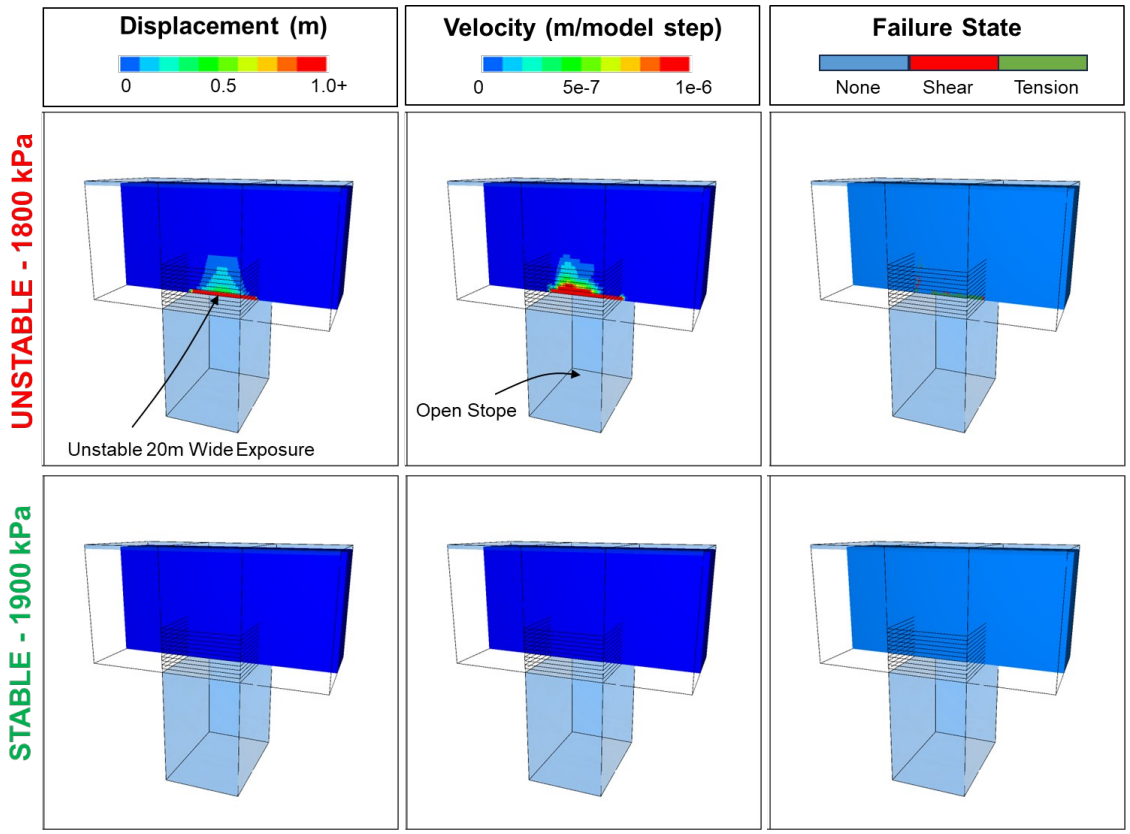

Figure 9. Example model results presented for 20 m stope span and 1 m beam heights.

A summary of all the simulation results compiled are presented in Figure 10. Note that results for repetitive cold joint locations (eg, stacked beams) are the same as those for a single beam, since depth of failure has not been considered in the definition of instability for this study. Furthermore, the failure mode may change between simulation sequences since the increase in beam thickness is more likely to result in a more complex failure mode that includes a combination of tension, flexure, and shear.

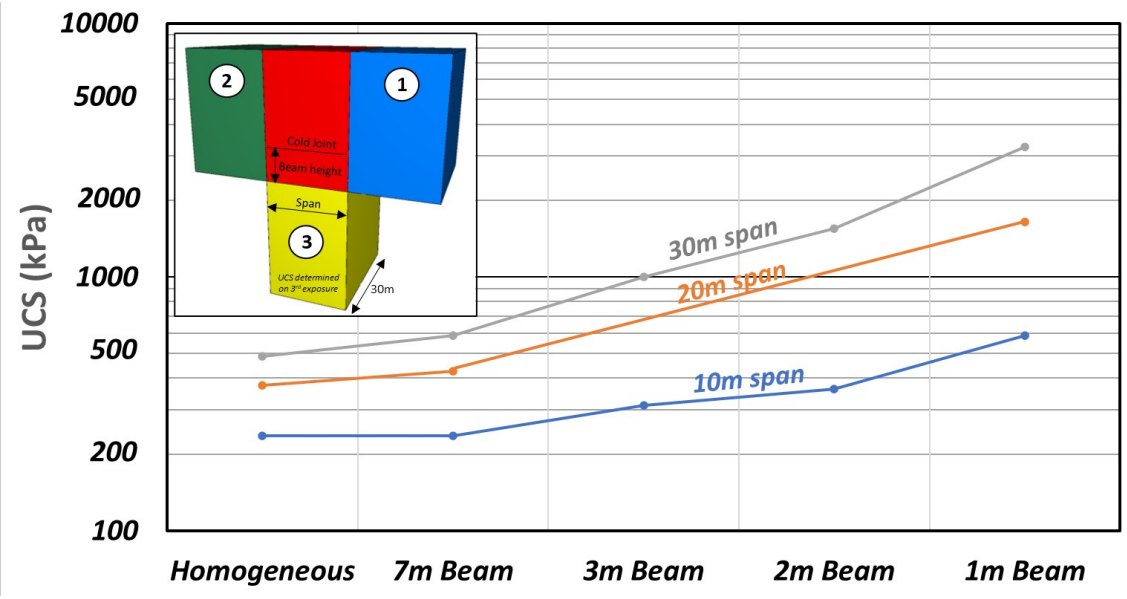

Figure 10. UCS required to maintain FOS 1 on third exposure with decreasing paste fill beam heights created by cold joints.

The normalised results in Figure 11 relate minimum strength required to maintain a FOS of 1 to the relative backfill beam height. The term Strength Factor has been defined to relate the design (homogeneous) strength of the CPB to the strength of the CPB with an internal cold joint. Span relates to the minimum stope dimension in the stope exposure regardless whether it is along or across strike.

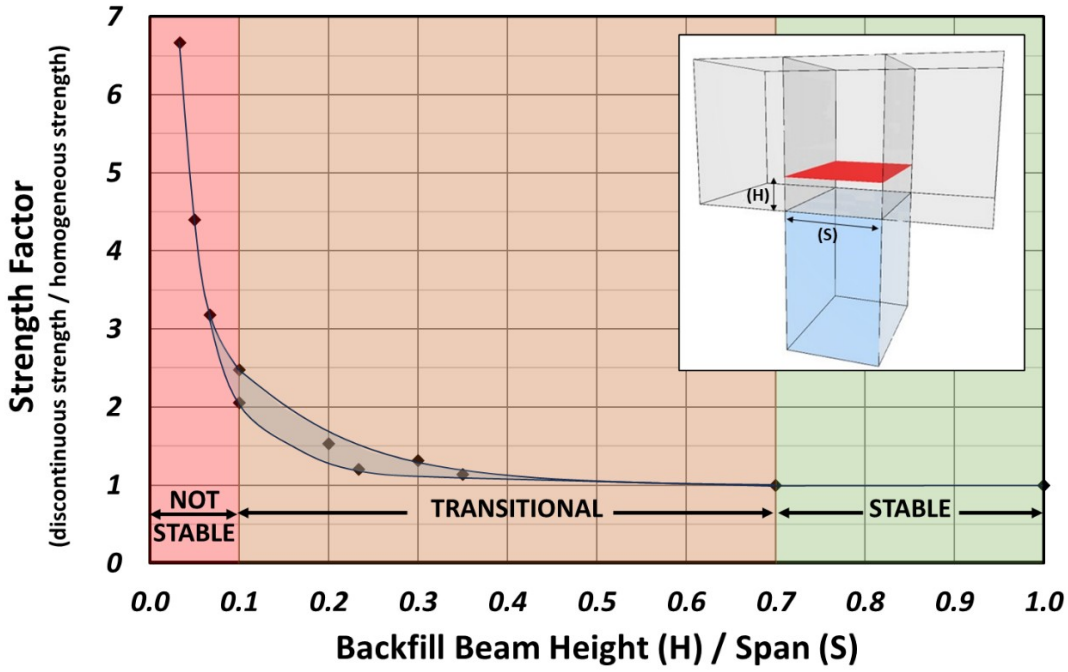

Figure 11. Normalised relationship between paste strength required to maintain FOS 1 and backfill beam height (H) relative to exposed span (S) for third exposure of stope.

Discussion

Typical CPB exposure design includes a FOS of 1.5. This FOS accounts for many factors including variations in batch dosing and variations in ambient curing conditions. When this FOS is applied to the presence of discontinuities formed during placement it is able to account for beam heights that are 0.15–0.25 the span width. The normalised relationship application can be used to determine the stability of a stope when a discontinuity has been formed or used to determine the minimum height of a plug pour as outlined in the following examples:

Example 1

A cold joint has formed during filling at a height of 4 m above the stope floor. The span of the stope on its third exposure is 12 m. This provides a H/S = 0.3. The strength factor can be determined to be 1.1–1.3. This is below 1.5 and suggest that the stope should still be stable if a FOS of 1.5 has been applied to the strength during design.

Example 2

Based on filling procedures, a cold joint beam height of 4 m occurs for all stopes. The planned exposed stope span is 30 m. This provides a H/S = 0.13. In order to negate the effect of the cold joint, the UCS of the CPB should be increased by a factor of 2 (or 200%) to maintain stability and reduce dilution.

It is noted that these examples are provided to indicate how the normalised relationship may be used by operational personnel to plan plug pours and/or provide guidance for expected dilution. This is provided as an indication of backfill stability and is in no way a suggestion that the strength of paste should be increased by up to 700% in the case of cold joints.

Conclusions

Laboratory testing on the direct tensile response of discontinues in CPB have been conducted. The results suggest that slick joints are stronger in tension than cold joints and provide a strength of approximately 5.6% of the UCS or 20% the homogenous direct tension response. Cold joints provide a tension strength of approximately 0.6% of the UCS or 2% of the homogenous direct tension response.

Strength responses were simulated in numerical exposure stability analysis for which the results have been generalised and are presented in a design chart. Based on the generalised results the following conclusions can be made:

- When a backfill beam height is greater than 70% of the span width, its presence is unlikely to cause instability issues. As such, it is advised that this value be considered as the minimum thickness of a continuous plug pour to minimise dilution.
- Significant instability is observed when backfill beam heights are less than 10% the stope span.

Acknowledgements

This research has been funded by Northern Star Resources Carouse Dam, Kanowna Belle and Thunderbox Mines; Agnico Eagle Fosterville Gold Mine (formerly Kirkland Lake Gold); BHP Prominent Hill (formerly Oz Minerals); Lundin Mining and Geotechnica.

Many thanks also to the Honors students at Deakin University who have contributed to the testing of cemented paste backfill, including Josh Phelan, Jordan Jones, Ahmad Albaba, Alex Hyland, Hamza Waqar, Rana Saim Ashraf, Abdul Rafay Imran, Maaz Salman, Shui (James) Chen, and Nathan Marley.

References

Alhussainy, F. et al. (2019) ‘A new method for direct tensile testing of concrete’, Journal of Testing and Evaluation, 47(2). Available at: https://doi.org/10.1520/JTE20170067.

Brackebusch, F. (1995) ‘Basics of paste backfill systems’, International Journal of Rock Mechanics and Mining Sciences and Geomechanics Abstracts, 32(3), p. 122A.
Brummer, R., Andrieux, P. and O’Connor, C. (2003) ‘Stability Analyses of Undermined Sill Mats for Base Metal Mining’, in B. et Al (ed.) Proceedings of the 3rd FLAC and Numerical Modelling in Geomechanics. Sudbury: A.A. Balkema, pp. 189–195.
Farrington, M. (2020) ‘Personal Communication’. Fosterville, Victoria, Australia: Fosterville Gold Mine.
Grabinsky, M., Jafari, M. and Pan, A. (2022) ‘Cemented Paste Backfill (CPB) Material Properties for Undercut Analysis’, Mining, 2(1), pp. 103–122. Available at: https://doi.org/10.3390/mining2010007.
Guo, L. et al. (2022) ‘Experimental Study on Direct Tensile Properties of Cemented Paste Backfill’, Frontiers in Materials, 9(March), pp. 1–10. Available at: https://doi.org/10.3389/fmats.2022.864264.
Hasan, A. et al. (2014) ‘In situ measurements of cemented paste backfilling in an operating stope at Lanfranchi Mine’, in Y Potvin & AG Grice (ed.) MineFill 2014 : Proceeding of the 11th International Symposium on Mining with Backfill. Perth: Australian Centre for Geomechanics, pp. 327–336. Available at: https://doi.org/10.36487/acg_rep/1404_26_hasan.
Hu, C. et al. (2020) ‘Physical investigation on the behaviours of voussoir beams’, Journal of Rock Mechanics and Geotechnical Engineering, 12(3), pp. 516–527. Available at: https://doi.org/10.1016/j.jrmge.2019.12.007.
Hughes, P.B. (2014) Design Guidelines: Underhand Cut and Fill Cemented Paste Backfill Sill Beams. University of British Columbia.
Itasca Consulting Group (2022) ‘FLAC3D 7.0 Explict Continuum Modeling of Non-Linear Material Behavior in 3D’. Minneapolis: Itasca Consulting Group.
Johnson, J.C. et al. (2015) ‘Strength and elastic properties of paste backfill at the Lucky Friday Mine, Mullan, Idaho’, 49th US Rock Mechanics / Geomechanics Symposium 2015, 3, pp. 2321–2332.
Koupouli, N., Belem, T. and Rivard, P. (2017) ‘Shear strength between cemented paste backfill and natural rock surface replicas’, in M. Hudyma and Y. Potvin (eds) Underground Mining Technology 2017. Perth: Australian Centre for Geomechanics, p. 375. Available at: https://papers.acg.uwa.edu.au/p/1710_29_Koupouli/.
Mitchell (1983) Earth Structures Engineering. Springer Dordrecht. Available at: https://doi.org/DOI https://doi-org.ezproxy-f.deakin.edu.au/10.1007/978-94-011-6001-8.
Mitchell, R.J. (1991) ‘Sill mat evaluation using centrifuge models’, Mining Science and Technology, 13(3), pp. 301–313. Available at: https://doi.org/10.1016/0167-9031(91)90542-K.
Nasir, O. and Fall, M. (2008) ‘Shear behaviour of cemented pastefill-rock interfaces’, Engineering Geology, 101(3–4), pp. 146–153. Available at: https://doi.org/10.1016/j.enggeo.2008.04.010.
Oulbacha, Z. (2014) Analyse numérique de la stabilité des piliers-dalles en remblai cimenté: une vérification des modèles de Mitchell. Ecole Polytechnique de Montreal. Available at: https://doi.org/10.13140/RG.2.2.15670.78408.
Pagé, P. et al. (2019) ‘Numerical investigation of the stability of a base-exposed sill mat made of cemented backfill’, International Journal of Rock Mechanics and Mining Sciences, 114(January), pp. 195–207. Available at: https://doi.org/10.1016/j.ijrmms.2018.10.008.
Pakalnis, R. et al. (2005) ‘Design spans-underhand cut and fill mining’, in Proceedings of 107th 107th CIM-AGM Toronto.
Pan, A.N. and Grabinsky, M.W.F. (2021) ‘Tensile strength of cemented paste backfill’, Geotechnical Testing Journal, 44(6), pp. 1886–1897. Available at: https://doi.org/10.1520/GTJ20200206.
Pan, A.N., Grabinsky, M.W.F. and Guo, L. (2021) ‘Shear Properties of Cemented Paste Backfill under Low Confining Stress’, Advances in Civil Engineering, 2021. Available at: https://doi.org/10.1155/2021/7561977.
Qi, C. et al. (2022) ‘Stability Evaluation of Layered Backfill Considering Filling’, Minerals, 12(271). Available at: https://doi.org/https://doi.org/10.3390/min12020271.
Rankine, R.M. and Sivakugan, N. (2007) ‘Geotechnical properties of cemented paste backfill from Cannington Mine, Australia’, Geotechnical and Geological Engineering, 25(4), pp. 383–393. Available at: https://doi.org/10.1007/s10706-006-9104-5.
Sainsbury, B. et al. (2024) ‘Characterisation of the geomechanical properties of cemented paste backfill for design’, in A. Fourie and D. Reid (eds) Proceedings of Pastefill 2024. Melbourne: Australian Centre for Geomechanics, Perth.
Sainsbury, B.L.L. and Sainsbury, D.P.P. (2017) ‘Practical Use of the Ubiquitous-Joint Constitutive Model for the Simulation of Anisotropic Rock Masses’, Rock Mechanics and Rock Engineering, 50(6), pp. 1507–1528. Available at: https://doi.org/10.1007/s00603-017-1177-3.

Sainsbury, D. and Sainsbury, B. (2014) 'Design and implementation of cemented rockfill at the Ballarat Gold Project', Mine Fill 2014 Proceeding of the 11th International Symposium on Mining with Backfill, pp. 1–12.
Sainsbury, D.P. et al. (2003) 'Investigation of the geomechanical criteria for safe and efficient crown pillar extraction beneath stabilised rockfill at the Crusader Mine', 10th ISRM Congress, pp. 1001–1006.
Sainsbury, D.P. and Cai, Y. (2001) 'Numerical analysis of crown pillar recovery techniques beneath paste fill', FLAC and Numerical Modeling in Geomechanics, pp. 295–301. Available at: https://doi.org/10.1201/9781003077527-44.
Sainsbury, D.P. and Urie, R. (2007) 'Stability Analysis of Horizontal and Vertical Paste Fill Exposures at the Raleigh Mine', in MINEFILL 2007 : Proceedings of the International Symposium on Mining with Backfill. Montreal, Quebec, CIM.
Shiels, A. and Sainsbury, D. (2020) 'Crown pillar extraction with paste underhand stoping', in Underground Mining Technology 2020 : Proceedings of the Second International Conference on Underground Mining Technology. Australian Centre for Geomechanics, Perth, pp. 217–230. Available at: https://doi.org/10.36487/acg_repo/2035_08.
Tesarik, D.R. et al. (2007) Numeric model of a cemented rockfill span test at the Turquoise Ridge Mine, Golconda, Nevada, USA.
Thompson, B.D.B., Bawden, W.F. and Grabinsky, M.W. (2012) 'In situ measurements of cemented paste backfill at the Cayeli mine', Canadian Geotechnical Journal, 49(7), pp. 755–772. Available at: https://doi.org/10.1139/T2012-040.

Acronyms

CPB	Cemented Paste Backfill
FOS	Factor of Safety
GSI	Geological Strength Index
UCS	Unconfined Compressive Strength